Complex Interaction Between Tori and Onset of Three-Frequency Quasi-Periodicity in a Current Mode Controlled Boost Converter

Damian Giaouris, Soumitro Banerjee, *Senior Member, IEEE*, Otman Imrayed, Kuntal Mandal, Bashar Zahawi, *Senior Member, IEEE*, and Volker Pickert, *Member, IEEE*

***Abstract*—It is known that power electronic circuits like dc-dc converters are highly nonlinear systems, and that period doubling and Neimark-Sacker bifurcations are common sources of instability in such systems. It has also been shown that these two types of bifurcation may interact, giving rise to interesting dynamical phenomena. In this paper we show that in a current mode controlled dc-dc converter, periodic, quasi-periodic, and saturation behavior can coexist for the same parameter value, and there can be complex interactions between them. Furthermore, abrupt exit to saturation mode can be triggered by a torus-torus collision. Finally, we report the first observation of three-frequency quasi-periodicity in a power electronic system.**

***Index Terms*—Dc-dc converters, fast scale instability, power electronics, slow scale instability.**

I. Introduction

POWER electronic circuits are normally designed to operate in a periodic steady state. The region in the parameter space where this behavior can be obtained is delimited by various instability conditions. The nature of these instabilities has been recently understood in terms of nonlinear dynamics.

In this approach, the periodic orbit is sampled in synchronism with the clock signal (called the Poincaré section), thus obtaining a discrete-time model or a map [1], [2]. The fixed point of the map signifies the periodic orbit, and its stability is given by the eigenvalues of the Jacobian matrix, computed at the fixed point. There are two basic ways in which such a periodic orbit may lose stability.

1) When an eigenvalue becomes equal to -1. The bifurcation is called a period-doubling bifurcation, which results in a period-2 orbit. This instability is not visible in an averaged model, and so it is also called a "fast-scale" instability [3]–[13].
2) When a pair of complex conjugate eigenvalues assume a magnitude of 1. This bifurcation is called a Neimark-Sacker bifurcation, which results in the onset of a slow sinusoidal oscillation in the state variables. The orbit rests on the surface of a torus. This instability can be predicted using the averaged model, and so it is also called the "slow-scale" instability [14]–[22].

In [23], [24], Chen, Tse, and others showed that dynamical behaviors resulting from these two types of bifurcations can interact, giving rise to interesting dynamics. In this paper we further investigate this phenomenon using the technique developed in [25]–[27]. In these earlier papers we used the monodromy matrix to determine the stability of a limit cycle and to design a supervising control law that guarantees a stable operation. In this paper we report the creation of a two-loop torus through a Neimark-Sacker bifurcation occurring on a period-2 orbit. There are complex interactions between periodic orbits, tori, and a saturation behavior, in which unstable tori play an important role. We have detected the unstable tori, and have demonstrated that the sudden departure from stable torus to a saturation behavior is caused by a collision between a stable and an unstable torus.

Also, in this system, under certain parameter choices a peculiar phenomenon is observed, in which a third frequency is generated and the waveform is modulated by this frequency. We find that this is *not* a beat phenomenon earlier reported in literature. In fact, the generation of the third frequency is the result of an instability of the torus, which is like a Neimark-Sacker bifurcation of the torus. This structurally stable three-frequency quasi-periodicity is generally very rare in nature, because small perturbations can destabilize the torus [28]. It is surprising to encounter this behavior in an electrical system, and this paper reports the first such observation. This phenomenon has been previously reported only in mechanical vibro-impacting systems [29]. For a more detailed exposure on torus bifurcations, see [30], [31].

The paper is organized as follows. In Section II we describe the system under study and its mathematical model. In the subsequent sections we present the bifurcation analysis of the system. We present the observation of a subcritical Neimark-Sacker bifurcation in Section III. The collision between a stable torus and an unstable torus, and the abrupt exit to the saturated behavior is investigated in Section IV. The observation of the Neimark-Sacker bifurcation of the torus and the onset of three-frequency quasi-periodicity is reported in

Manuscript received December 16, 2010; revised March 16, 2011; accepted June 08, 2011. This paper was recommended by Associate Editor M. Di Marco

D. Giaouris, O. Imrayed, B. Zahawi, and V. Pickert are with the School of Electrical, Electronic and Computer Engineering, Newcastle University, Merz Court, Newcastle upon Tyne NE1 7RU, U.K. (e-mail: Damian.Giaouris@newcastle.ac.uk).

S. Banerjee is with the Indian Institute of Science Education & Research—Kolkata, Mohanpur Campus, Nadia 741252, India.

K. Mandal is with the Indian Institute of Technology, Kharagpur 721302, India.

Color versions of one or more of the figures in this paper are available online at http://ieeexplore.ieee.org.

Digital Object Identifier 10.1109/TCSI.2011.2161371

This article has been accepted for inclusion in a future issue of this journal. Content is final as presented, with the exception of pagination.

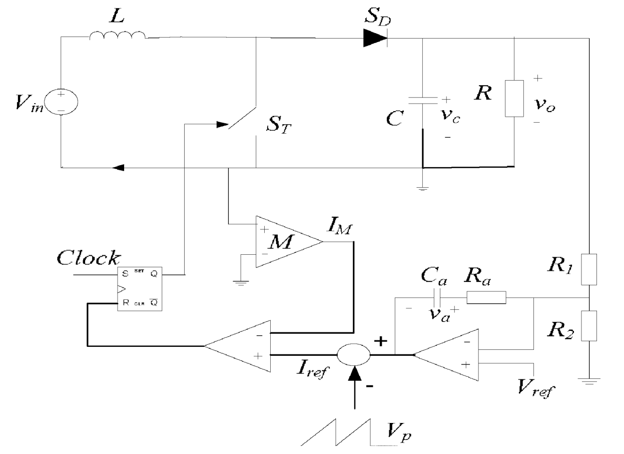

Fig. 1. Schematic diagram of the current mode controlled boost converter. The nominal parameter value taken in this study are $V_{\rm in} = 2.9 - 25$ V, $R = 20 - 30\ \Omega$, $L = 165\ \mu$H, $r_L = 0.04\ \Omega$, $C = 150\ \mu$F, $r_C = 0.03\ \Omega$, $r_T = 0.055\ \Omega$, $r_D = 0.01\ \Omega$, $T = 40\ \mu$s, $V_{\rm ref} = 2.5$ V, $R_1 = 47$ kΩ, $R_2 = 6.8$ kΩ, $R_a = 10$ kΩ, $C_a = 2.2$ nF, $V_p = 0.445$ V, $M = 0.3$ V/A.

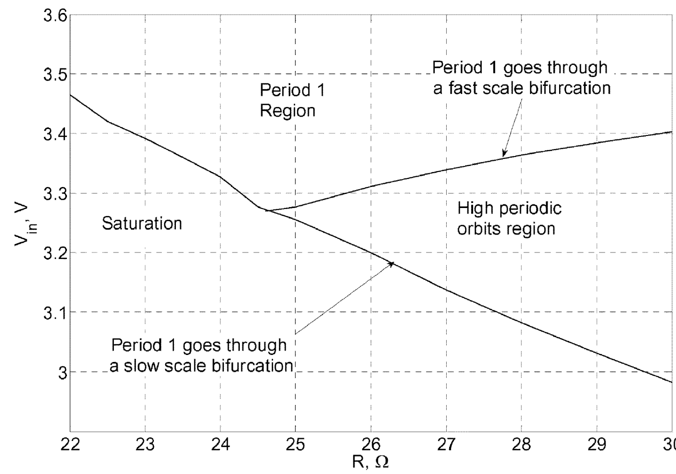

Fig. 2. Two-parameter bifurcation diagram.

Section V. We have used the second-order Poincaré map [31], [32] to investigate such instabilities of a quasi-periodic orbit. In this technique a second Poincaré section is placed in the discrete-time state space to investigate the stability of a torus. The results of the application of this method is presented in Section VI.

II. The Boost Converter and Its Mathematical Model

The schematic diagram of the current mode controlled boost converter is shown in Fig. 1. The switch S_T is turned on by a free running clock. When the switch S_T is on, the inductor current i_L rises, and it is switched off when i_L reaches a reference value $I_{\rm ref}$. This reference current signal is generated through output voltage feedback, using a PI controller and a compensation ramp.

Considering the state vector $x = [i_L\ v_c\ v_a]^T$, the mathematical model is given by [23], [24]

$$\dot{x} = \begin{cases} A_1 x + BV_{\rm in}, & \text{for } S_T = \texttt{ON} \text{ and } S_D = \texttt{OFF} \\ A_2 x + BV_{\rm in}, & \text{for } S_T = \texttt{OFF} \text{ and } S_D = \texttt{ON} \end{cases} \quad (1)$$

with

$$A_1 = \begin{bmatrix} -\frac{r_L + r_T}{L} & 0 & 0 \\ 0 & -\frac{1}{\tau_m(1+k_c)} & 0 \\ 0 & \frac{g}{\tau_a(1+k_c)} & 0 \end{bmatrix}, \quad B = \begin{bmatrix} \frac{1}{L} \\ 0 \\ -\frac{g k_d V_{\rm ref}}{\tau_a V_{\rm in}} \end{bmatrix}$$

$$A_2 = \begin{bmatrix} -\frac{r_L + r_D}{L} - \frac{r_c}{L(1+k_c)} & -\frac{1}{L(1+k_c)} & 0 \\ \frac{1}{C(1+k_c)} & -\frac{1}{\tau_m(1+k_c)} & 0 \\ \frac{g r_c}{\tau_a(1+k_c)} & \frac{g}{\tau_a(1+k_c)} & 0 \end{bmatrix}$$

and $k_c = r_c/R$, $g = R_a/R_1$, $\tau_m = RC$, $\tau_a = R_a C_a$, $k_d = (R_1 + R_2)/R_2$, r_T is the switching resistance, r_L internal resistance of the inductor, r_C is the resistance of the capacitor, and r_D is the diode resistance.

In the normal operating condition, the state variables of the converter follow a period-1 orbit. But, with the variation of the external parameters like the input voltage or the load resistance, this orbit may become unstable, and other dynamical modes may come into operation.

It has been shown earlier [25]–[27] that the stability of such an orbit can be assessed by computing the state transition matrix over a complete clock cycle (called the monodromy matrix), which, in turn, is composed of the state transition matrices over the ON and OFF periods and those across the switching events (called the saltation matrices). The orbit is stable if the eigenvalues of the monodromy matrix are inside the unit circle.

It has to be noted that the stability analysis presented in this paper is based on the eigenvalues of the invariant sets (limit cycles, fixed points, and tori) and not on a normal form representation of the system [30]. We chose this approach as it is considered to be more common in power electronic circuits [1], [33].

In the two-dimensional parameter plane ($V_{\rm in}$ versus R) the positions of the bifurcation lines corresponding to fast-scale and slow-scale instabilities of the period-1 orbit are shown in Fig. 2. It is seen that there exists a region where the nominal period-1 orbit is stable. It is bounded by a line representing the onset of a fast-scale instability and a line representing the onset of a slow-scale instability. If we vary the parameter across the second line, we find that the post-instability behavior diverges, and the system goes into saturation. There is however a region where the period-2 behavior undergoes the Neimark-Sacker bifurcation, and there is interaction between a fast-scale and a slow-scale bifurcation. In this paper we mainly focus on the dynamics resulting from this interaction.

III. Subcritical Neimark-Sacker Bifurcation

From Fig. 2 we expect that at $R = 24\ \Omega$, if the parameter $V_{\rm in}$ is slowly reduced, a stable fixed point would undergo a Neimark-Sacker bifurcation. In this section we probe this phenomenon closely.

As the parameter $V_{\rm in}$ is reduced, the eigenvalues of the period 1 orbit were calculated using the technique developed in [25]–[27] and are shown in Table I. It shows that a complex conjugate pair of eigenvalues went out of the unit circle at $V_{\rm in} = 3.322$ V, which marks a Neimark-Sacker bifurcation. But for $V_{\rm in} > 3.322$ V, the saturation behavior also exists as a coexisting attractor which could be reached from a set of initial conditions (see Fig. 3). The basins of attraction of the two attractors

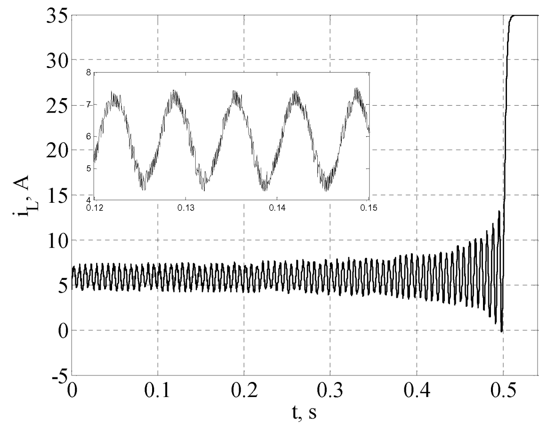

Fig. 3. Time response for $R = 24$ V and $V_{\rm in} = 3.32$ V, showing the exit to the saturation behaviour.

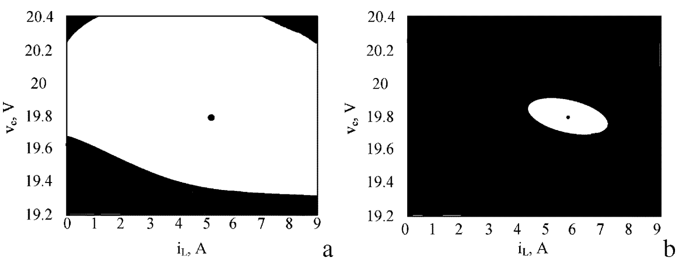

Fig. 4. The white area corresponds to the region of attraction of the period-1 orbit, while the basin of attraction of the saturated behavior is represented by black. (a) $V_{\rm in} = 3.5$ V. (b) $V_{\rm in} = 3.33$ V.

TABLE I
FLOQUET MULTIPLIERS OF THE PERIOD 1 ORBIT FOR $R = 24\ \Omega$

$V_{\rm in}, V$	duty cycle	λ_1	$\lambda_{2,3}$	$\lvert\lambda_{2,3}\rvert$
3.50	0.8483	-0.9609	$0.9978 \pm 0.0398j$	0.9986
3.45	0.8514	-0.9684	$0.9982 \pm 0.0393j$	0.9970
3.40	0.8535	-0.9759	$0.9986 \pm 0.0388j$	0.9993
3.38	0.8557	-0.9789	$0.9988 \pm 0.0386j$	0.9995
3.36	0.8570	-0.9818	$0.9989 \pm 0.0384j$	0.9996
3.34	0.8582	-0.9847	$0.9991 \pm 0.0381j$	0.9998
3.325	0.8592	-0.9869	$0.9992 \pm 0.0380j$	0.9999
3.322	0.8595	-0.9876	$0.9993 \pm 0.0379j$	1

are shown in Fig. 4. In order to draw the region of attractions we fixed the value of the 3rd state to a constant value. This value was found by locating the plane where the invariant torus lies (using a simple equation $ax + by + cz = d$) and then choosing the initial conditions from the plane. While operating in the stable period-1 orbit, if the state is perturbed (due to noise or other means) beyond its basin of attraction, the converter would operate in a saturation mode even though the parameter values indicate that the period-1 behavior is stable.

These two stable behaviors are separated in the state space by an unstable torus (a closed loop in discrete time) that is born at $V_{\rm in} \approx 3.322$ V in a *subcritical* Neimark-Sacker bifurcation. The situation becomes clearer when we plot the bifurcation diagram including the unstable orbits (Fig. 5). As the parameter is reduced, the unstable torus collapses onto the stable period 1 orbit marking the onset of a subcritical Neimark-Sacker bifurcation. This explains why, as the paremeter is smoothly reduced, the orbit abruptly jumps from the period-1 stable behavior to the undesirable saturated behavior at $V_{\rm in} \approx 3.32$ V.

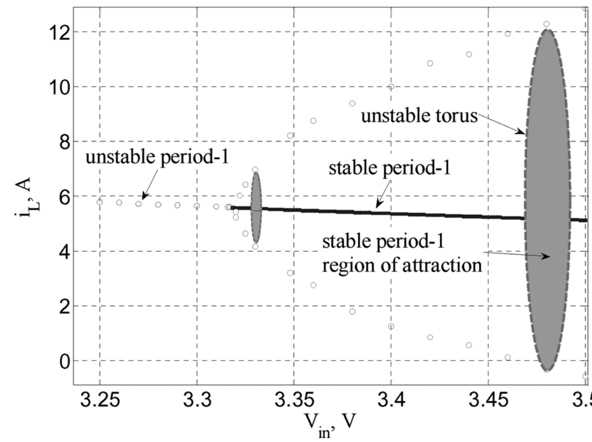

Fig. 5. Bifurcation diagram for $R = 24\ \Omega$ showing the unstable torus collapsing to the stable period 1 attractor at $V_{\rm in} = 3.322$ V.

IV. COLLISION BETWEEN TORI

According to Fig. 2 for $R = 26\ \Omega$ if the parameter $V_{\rm in}$ is reduced continuously, we expect to go from period 1 to period 2 through a period doubling bifurcation. As the parameter is further reduced, at some point there will be a slow-scale bifurcation. The period-2 orbit may bifurcate further (leading to period-4, period-8, or higher periodic orbit), before the slow-scale bifurcation occurs. In this section we focus on this sequence of events, and the resulting global dynamics.

A typical bifurcation diagram in this range is shown in Fig. 6. As the parameter is reduced, there is a period doubling bifurcation at $V_{\rm in} = 3.3105$ V (The duty ratio is 0.8575 and the eigenvalues are -1.0000 and $0.9983 \pm 0.0384j$), followed by a Neimark-Sacker bifurcation of the period 2 orbit at $V_{\rm in} = 3.3058$ V. At that parameter value, the duty ratios of the two cycles in a period are 0.9715 and 0.7441, and the eigenvalues of the period-2 orbit are 0.9969, and $0.9996 \pm 0.0754j$ with modulus 1.0000. Following the latter bifurcation, the situation in the discrete-time state space is as follows. There is an unstable period-1 fixed point with a stable two-dimensional manifold and an unstable one-dimensional manifold. The unstable manifold reaches out to the two unstable period-2 points. Each of these points has a stable one-dimensional manifold and an unstable two-dimensional manifold on which the stable quasi-periodic behavior lies. Thus, each point of the period-2 orbit is surrounded by a closed loop representing the torus. The situation is depicted in Fig. 7, obtained by placing an initial condition very close to the stable two-dimensional manifold of the unstable period-1 fixed point, and observing the iterates.

The torus created at this bifurcation expands fast and soon the expansion is arrested as it hits a nonsmoothness boundary. So far all the bifurcations were smooth in nature, and there was one switching cycle in each clock cycle. At this point cycles begin to be skipped without switching (see Fig. 8).

As the parameter is further reduced, at $V_{\rm in} \approx 3.3031$ V the unstable period-2 orbit becomes stable at a border collision (see Fig. 9), i.e., for $V_{\rm in} > 3.3031$ V every clock cycle contains a switching while for $V_{\rm in} < 3.3031$ V every alternate cycle is skipped without switching. Hence in the range $V_{\rm in} = [3.3, 3.2371]$ we have an unstable period-1 fixed point,

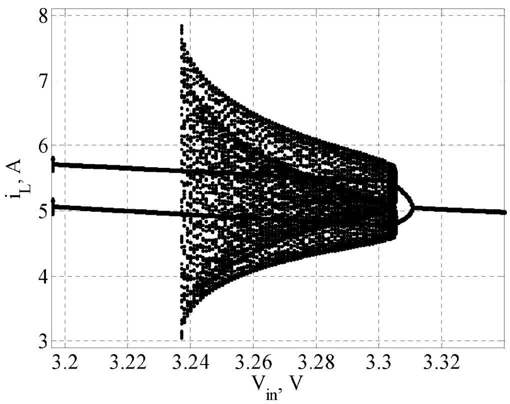

Fig. 6. Bifurcation diagram for $R = 26\ \Omega$.

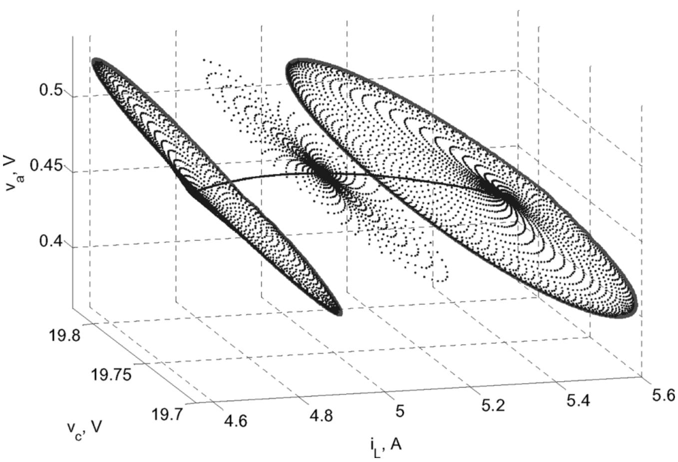

Fig. 7. System's response at $V_{\rm in} = 3.3032$ V, $R = 26\ \Omega$ starting from an initial condition close to the stable manifold of the period-1 fixed point.

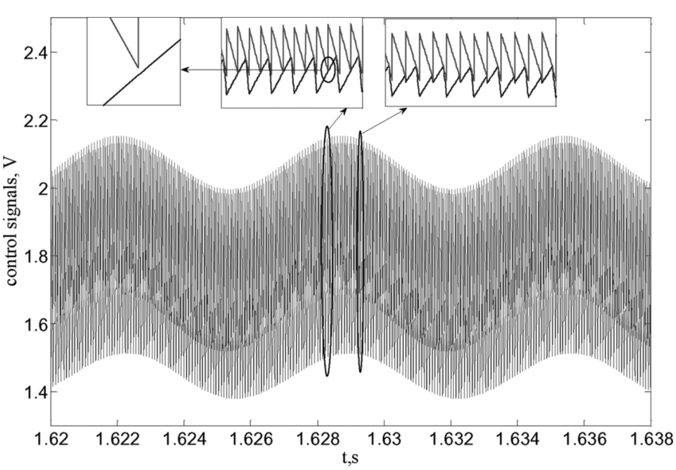

Fig. 8. Waveform of the control signal showing the border collision (onset of skipped cycles) that arrested the expansion of the quasi-periodic orbit; $V_{\rm in} = 3.3053$ V, $R = 26\ \Omega$.

a stable period-2 fixed point, a stable torus, the saturation attractor, and 2 unstable tori—one that separates the stable period-2 orbit from the stable torus and one that separates the stable torus from the saturation attractor. These orbits and the basins of attraction are shown in Fig. 10.

An interesting event unfolds as the parameter is reduced further, to around $V_{\rm in} \approx 3.2371$ V, when the orbit diverges to the saturation attractor. Our investigation revealed that as the

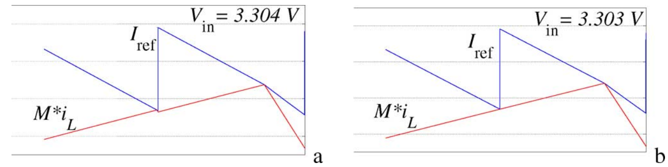

Fig. 9. The waveforms of $I_{\rm ref}$ and the control voltage $M * i_L$ at $R = 26\ \Omega$: (a) the waveform of the unstable period-2 orbit for $V_{\rm in} = 3.304$ V (obtained by locating the unstable fixed point of the Poincaré map by the technique described in [34]), (b) the waveform of the stable period-2 orbit for $V_{\rm in} = 3.303$ V, showing the border collision (onset of skipped cycles) that stabilized the unstable period-2 orbit. The eigenvalues jumped from 0.995689 and $0.997847 \pm 0.074884j$ (modulus 1.000653) to -0.974107 and $0.995375 \pm 0.076896j$ (modulus 0.998341) as a result of the border collision.

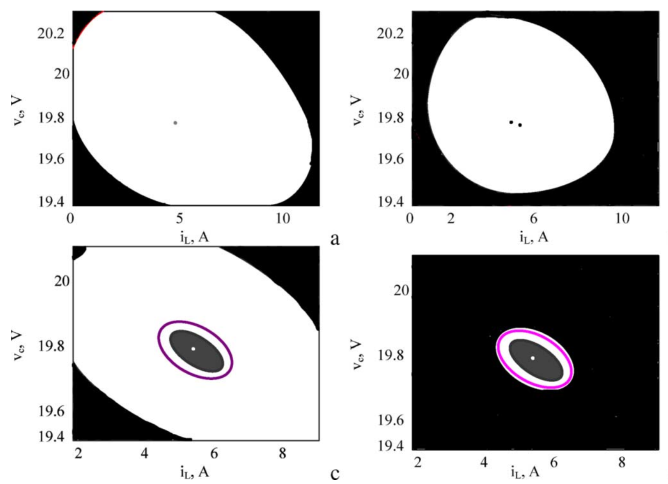

Fig. 10. Regions of attraction for $R = 26\ \Omega$, (a) $V_{\rm in} = 3.34$: a stable period 1 orbit, a saturation attractor, and an unstable torus whose stable manifold forms the basin boundary, (b) $V_{\rm in} = 3.308$: a stable period-2 orbit, a saturation attractor, and an unstable torus forming the basin boundary, (c) $V_{\rm in} = 3.26$: a stable period-2 fixed point, a stable torus, the saturation attractor and two unstable tori dividing the basins of attraction, (d) $V_{\rm in} = 3.2371$: as before but just before the torus-torus collision. The attractors in (a) and (b) are represented by their T-return maps while in (c) and (d) by their $2T$-return maps.

parameter approaches this value, the second stable torus and the unstable torus approach each other and at that parameter value they merge and disappear. This event is reminiscent of a saddle-node bifurcation, where the participating orbits are a stable torus and an unstable torus. After this event, any initial condition outside the first unstable torus diverges to the saturation attractor.

V. Three-Frequency Quasi-Periodicity

Based on Fig. 2 we do not expect any qualitative change in the bifurcation behavior in the range from $R = 24.5\ \Omega$ (the codimension-2 bifurcation point) and $R = 26\ \Omega$. Yet, when the one-parameter bifurcation diagram is plotted along the section $R = 25.1\ \Omega$ (Fig. 11), we see an interesting phenomenon at $V_{\rm in} \approx 3.267$ V, just before the torus-torus collision. Looking at the two-dimensional T-sampled trajectory (Fig. 12) we see that at $V_{\rm in} = 3.268$ V there are two loops around the two points of the unstable period-2 orbit. When the parameter is reduced to $V_{\rm in} = 3.266$ V, the discrete-time picture itself takes the shape of a torus. The spectrum (Fig. 13) reveals that at this point a third frequency component is added, and hence the behavior is

This article has been accepted for inclusion in a future issue of this journal. Content is final as presented, with the exception of pagination.

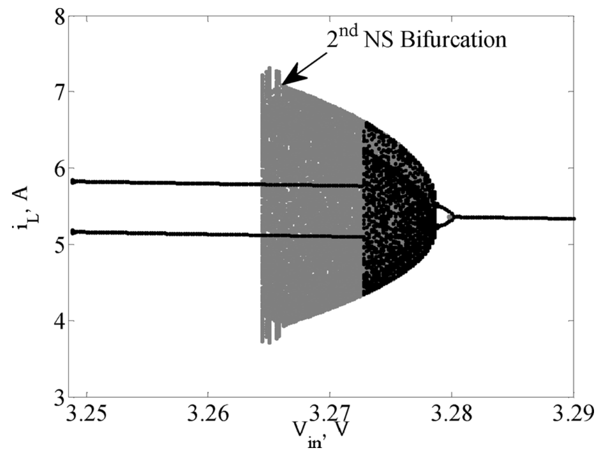

Fig. 11. Bifurcation diagram for $R = 25.1\ \Omega$.

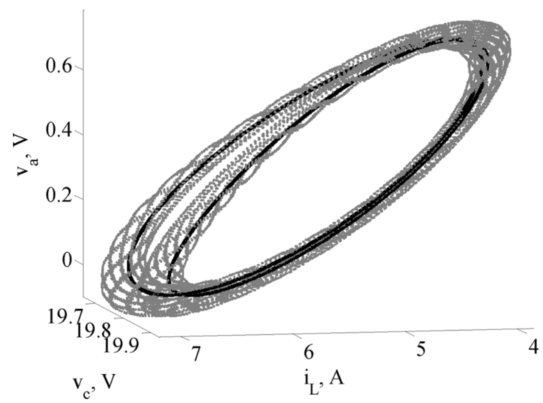

Fig. 12. Trajectories for $V_{\text{in}} = 3.268$ V (in black) and $V_{\text{in}} = 3.266$ V (in gray) sampled every T seconds.

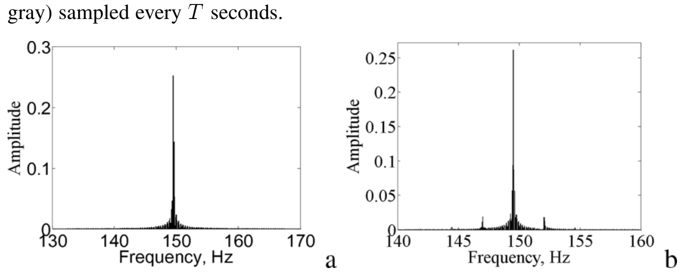

Fig. 13. Frequency spectra for $R = 25.1\ \Omega$, (a) for $V_{\text{in}} = 3.268$ V and (b) for $V_{\text{in}} = 3.266$ V.

a three-frequency quasi-periodicity with two loops. Such a dynamical behavior is extremely rare in nature, and to our knowledge this is the first time it has been found in an engineering system.

As the parameter is further reduced, the three-frequency torus is destroyed when it collides with the unstable torus, as shown in Fig. 14.

VI. Investigation Using a Second Poincaré Section

In order to investigate the phenomena reported in Sections IV and V, we adopt the technique of second Poincaré section [35]–[37]. The system is time driven with periodicity T, and the objects under study are two-loop tori. In order to concentrate on one of them, we sample the trajectory at every $2T$ seconds, thus obtain points on the Poincaré section that form one loop. Our intention is to study the stability and bifurcation of this quasi-periodic behavior.

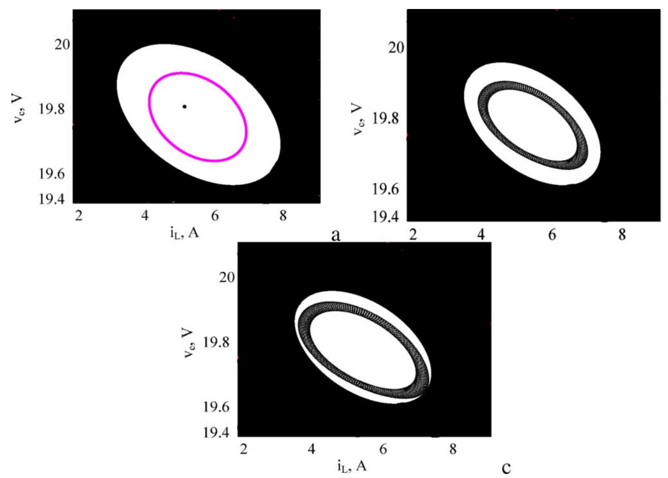

Fig. 14. Regions of attraction for $R = 25.1\ \Omega$ and (a) $V_{\text{in}} = 3.268$ V and (b) $V_{\text{in}} = 3.267$ V and $V_{\text{in}} = 3.266$ V, sampled at 2T.

Now we place a "second Poincaré section" (say, at $i_L = 5.5$ A) to intersect the closed curve on which the points of the $2T$-sampled quasi-periodic orbit fall (Fig. 15). Thus, the procedure involves a combination of a stroboscopic section obtained using the $2T$ map, and a standard Poincaré section. Since the points in general would not fall on this plane, we take three points before and three points after the crossing, and use a spline interpolation. We thus obtain the point where the curve passing through the discrete-time trajectory intersects the second Poincaré section. For the stable quasi-periodic orbit, this procedure yields a fixed point in steady state.

Now we assume that the dynamics on this second Poincaré section, in the neighborhood of the fixed point, is given by a linear equation of the form

$$\mathbf{x}_{n+1} = \mathbf{A}\mathbf{x}_n,$$

where $\mathbf{x}$ represents the deviation from the fixed point. In order to assess the stability of the quasi-periodic orbit, we need to evaluate the Jacobian matrix $\mathbf{A}$ at the fixed point. If we place the second Poincaré section on a point of the quasi-periodic drift ring, the iterates starting from that point go around the loop and cross the same point 83 iterates later. In order to calculate the stability of the whole quasi-periodic orbit, we have to multiply the state transition matrices across each of these 83 clock cycles. The state transition matrix across a whole clock cycle is called a "monodromy matrix" which is the product of the exponential matrices for the ON and OFF periods and the saltation matrices across the switching events [25], [26] occurring in that cycle. We calculated the time durations spent in the ON and OFF phase in each cycle, and thus calculated the monodromy matrix in each cycle. The product of the 83 monodromy matrices gives the local linear approximation around the fixed point on the second Poincaré section. The eigenvalues of this Jacobian matrix gives the stability of the fixed point.

Table II shows the eigenvalues thus obtained, as the parameter is reduced to the bifurcation value. It is clearly seen that the eigenvalues are complex conjugate, and the magnitude approaches unity as the parameter value of $V_{\text{in}} = 3.268$ V is approached.

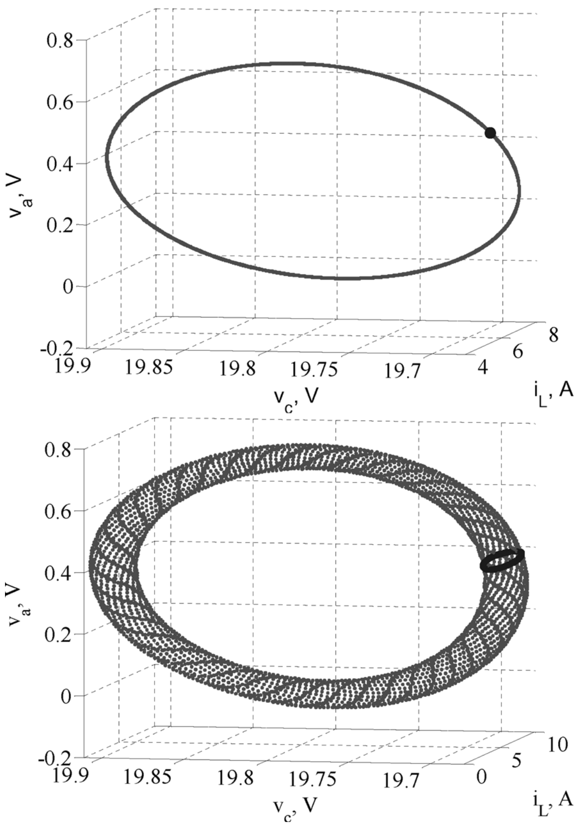

Fig. 15. The twice sampled state space, once at $2T$ and once when $i_l = 5.5$ A. Top: when the torus is stable, for $V_{\rm in} = 3.268$ V, bottom: when the three-frequency torus develops, for $V_{\rm in} = 3.267$ V.

TABLE II
EIGENVALUES OF THE FIXED POINT ON THE SECOND POINCARÉ SECTION. IT SHOWS THAT THE NEIMARK-SACKER BIFURCATION OF THE TORUS OCCURS AT $V_{\rm in} \approx 3.268$ V

$V_{\rm in}$	Eigenvalues	Absolute Value
3.271	$0.9822015 \pm 0.1133319j$	0.9887184
3.270	$0.9830253 \pm 0.1449007j$	0.9936473
3.269	$0.9848370 \pm 0.1431570j$	0.9951873
3.268	$0.9931656 \pm 0.1123643j$	0.9995017

In order to check the result, we gave a purturbation in the initial condition. Since the torus is now stable, the iterates will go around the torus and will move progressively closer to it. We record the subsequent intersections with the second Poincaré section, which are shown in Fig. 16. Using the positions of two such piercing points, one can obtain the matrix $\mathbf{A}$, and its eigenvalues. The eigenvalues obtained this way are very close to the ones shown in Table II. Therefore we conclude that, as $V_{\rm in}$ is reduced, the complex conjugate eigenvalues approach a magnitude of unity, and at the bifurcation point, the magnitude becomes unity.

Fig. 15 shows that before the onset of this instability, the second Poincaré section could see one point. After the onset of this instability a loop develops. This suggests that a Neimark-Sacker type bifurcation took place on the already existing torus.

In case of the torus-torus collision described in Section IV, we applied the method of second Poincaré section. In this case there is no rotation, and the iterates approach the fixed point along a linear path (which indicates that the eigenvalues should be real and positive). The Jacobian matrix $\mathbf{A}$ was again calculated as a product of 84 monodromy matrices, and the resulting evolution of the eigenvalues is tabulated in Table III.

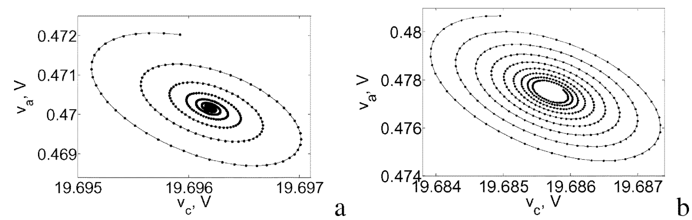

Fig. 16. Second Poincaré points. (a) $V_{\rm in} = 2.271$ V, (b) $V_{\rm in} = 2.269$ V.

TABLE III
EIGENVALUES OF THE FIXED POINT ON THE SECOND POINCARÉ SECTION, AS THE TORUS-TORUS COLLISION IS APPROACHED

$V_{\rm in}$	Eigenvalues		
3.28	0.95028922971,	0.94403283208,	−0.95822348419
3.26	0.98728655092,	0.96036314168,	−0.94614257837
3.25	0.99165802082,	0.97522880046,	−0.92296425403
3.24	0.99965802082,	0.98107914455,	−0.84362481946

From this table it is clear that one eigenvalue approaches $+1$ as the parameter approaches the bifurcation value. Thus, this bifurcation is torus equivalent of the saddle-node bifurcation, at which a node and a saddle on the second Poincaré section merge and disappear. In the state space we observe the merging of a stable torus and an unstable torus, and the disappearance of both.

VII. PROPAGATION OF NEIMARK-SACKER BIFURCATIONS

Another interesting phenomenon is noticed if the eigenvalues of the orbits are calculated along the bifurcation diagrams in Figs. 5, 6, and 11. We find that where the unstable period-1 orbit goes through a Neimark-Sacker bifurcation (i.e., two complex conjugate eigenvalues assume a magnitude of 1), the higher periodic orbits that had resulted from the period doubling bifurcations also undergo a similar event (of course there is a possibility that the two phenomena do not occur at the same instant as our analysis is restricted due to numerical inaccuracies). For example, in the case of Fig. 11 ($R = 25.1\ \Omega$), the period-1 orbit bifurcated into a period-2 orbit at $V_{\rm in} \approx 3.28$ V. Following the unstable period-1 orbit, we find that at $V_{\rm in} = 3.250$ V the Floquet multipliers assume the values -1.005, $0.9993 \pm 0.0375j$ (the absolute value and phase of the complex multipliers are 1 and 0.0375 radians respectively). At the same parameter value, if we calculate the Floquet multipliers of the period-2 orbit, we find them to be -0.9759, $0.9972 \pm 0.0753j$ (the absolute value and phase of the complex eigenvalues are 1 and 0.0754 radians respectively). At this point we see the onset of another two-loop torus. This implies that the instability of the period-1 orbit along the eigenplane associated with the complex eigenvalues propagates to the period-2 orbit, and induces a similar instability in that orbit also. If the period-2 orbit had further bifurcated before the onset of the Neimark-Sacker bifurcation, the same phenomenon would be seen in the resulting high-periodic orbit.

VIII. CONCLUSIONS

We have investigated the dynamics of a current mode controlled boost converter which exhibits both fast-scale and slow-scale instabilities. We focused our attention on the parameter ranges where the dynamics resulting from these two types of instabilities interact.

In this system there is a range of the parameters where the dynamics abruptly change from a period-1 behavior to a saturation behavior at a bifurcation point. We have shown that this behavior is caused by a subcritical Neimark-Sacker bifurcation.

In another parameter range, a fast-scale (period doubling) bifurcation is followed by a supercritical Neimark-Sacker bifurcation occurring in the period-doubled orbit. This results in a two-loop torus. Subsequently the unstable period-2 orbit becomes stable through a border collision bifurcation. In that situation there are three attractors: the two-loop torus, the period-2 orbit, and the saturation attractor. These three stable behaviors are enclosed in their own basins of attraction, which are separated by two unstable tori. As the parameter is varied, a pair of stable and unstable tori collide and disappear. The observable signature of this event is an abrupt exit to the saturation behavior.

We have also demonstrated a new type of dynamics where a third frequency is spontaneously generated in the system, and the waveform is modulated by this slow frequency component. This three-frequency quasi-periodicity is an extremely rare phenomenon in nature, and has been reported for the first time in an engineering system.

In investigating the stability of quasi-periodic orbits, and in understanding the bifurcations occurring on the tori, we have adoped the method of second Poincaré section. In this approach we place a second Poincaré section to intersect the closed loop on which the points obtained through stroboscopic sampling lie. In that plane, the quasi-periodic orbit would be represented by a fixed point. We have presented a method of obtaining the Jacobian matrix at the fixed point. Calculation of the eigenvalues of the Jacobian matrix indicates that the generation of the three-frequency quasi-periodicity is caused by another Neimark-Sacker type bifurcation (complex conjugate eigenvalues reaching the unit circle) occurring on the torus, while the collision of the stable and unstable tori is akin to the saddle-node bifurcation (one eigenvalue reaching $+1$) where the participating orbits are tori instead of fixed points.

Finally, we have shown that a Neimark-Sacker bifurcation can propagate from a period-1 orbit to the orbits that result from period-doubling of that orbit.

References

[1] S. Banerjee and G. C. Verghese, Eds., *Nonlinear Phenomena in Power Electronics: Attractors, Bifurcations, Chaos, and Nonlinear Control*. New York, IEEE Press, 2001.

[2] C. K. Tse, *Complex Behavior of Switching Power Converters*. Boca Raton, FL: CRC, 2003.

[3] K. Chakrabarty, G. Poddar, and S. Banerjee, "Bifurcation behaviour of the buck converter," *IEEE Trans. Power Electron.*, vol. 11, pp. 439–447, May 1996.

[4] S. Banerjee and K. Chakrabarty, "Nonlinear modeling and bifurcations in the boost converter," *IEEE Trans. Power Electron.*, vol. 13, no. 2, pp. 252–260, 1998.

[5] J. H. B. Deane and D. C. Hamill, "Instability, subharmonics, and chaos in power electronics circuits," *IEEE Trans. Power Electron.*, vol. 5, pp. 260–268, Jul. 1990.

[6] D. C. Hamill and J. H. B. Deane, "Modeling of chaotic DC-DC converters by iterated nonlinear mappings," *IEEE Trans. Power Electron.*, vol. 7, pp. 25–36, Jan. 1992.

[7] M. di Bernardo and F. Vasca, "Discrete-time maps for the analysis of bifurcations and chaos in DC/DC converters," *IEEE Trans. Circuits Syst. I, Fundam. Theory Appl.*, vol. 47, no. 2, pp. 130–143, 2000.

[8] M. D. Bernardo, F. Garofalo, L. Glielmo, and F. Vasca, "Switchings, bifurcations and chaos in DC-DC converters," *IEEE Trans. Circuits Syst. I, Fundam. Theory Appl.*, vol. 45, no. 2, pp. 133–141, 1998.

[9] M. D. Bernardo, C. Budd, and A. Champneys, "Grazing, skipping and sliding: Analysis of the non-smooth dynamics of the DC-DC buck converter," *Nonlinearity*, vol. 11, no. 4, pp. 858–890, 1998.

[10] S. Kapat, S. Banerjee, and A. Patra, "Discontinuous map analysis of a DC-DC converter governed by pulse skipping modulation," *IEEE Trans. Circuits Syst. I, Reg. Papers*, vol. 57, pp. 1793–1801, Jul. 2010.

[11] F. Xie, R. Yang, and B. Zhang, "Bifurcation and border collision analysis of voltage-mode-controlled flyback converter based on total ampere-turns," *IEEE Trans. Circuits Syst. I, Reg. Papers* 2011 [Online]. Available: http://ieeexplore.ieee.org/xpl/freeabs_all.jsp?arnumber=5729352

[12] M. Li, C. Tse, H. Iu, and X. Ma, "Unified equivalent modeling for stability analysis of parallel-connected DC/DC converters," *IEEE Trans. Circuits Syst. II, Exp. Briefs*, vol. 57, pp. 898–902, Nov. 2010.

[13] A. E. Aroudi, E. Rodriguez, R. Leyva, and E. Alarcon, "A design-oriented combined approach for bifurcation prediction in switched-mode power converters," *IEEE Trans. Circuits Syst. II, Exp. Briefs*, vol. 57, pp. 218–222, Mar. 2010.

[14] A. E. Aroudi, L. Benadero, E. Toribio, and S. Machiche, "Quasiperiodicity and chaos in the DC-DC buck-boost converter," *Int. J. Bifurcation Chaos*, vol. 10, no. 2, pp. 359–371, 2000.

[15] C. K. Tse, Y. M. Lai, and H. H. C. Iu, "Hopf bifurcation and chaos in a free-running autonmous Ćuk converter," *IEEE Trans. Circuits Syst. I, Fundam. Theory Appl.*, vol. 47, pp. 448–457, Apr. 2000.

[16] H. Iu, C. Tse, V. Pjevalica, and Y. Lai, "Analysis of Hopf bifurcation in parallel-connected boost converters via averaged models," in *Proc. IEEE Int. Symp. Circuits Syst. (ISCAS)*, 2002, vol. 5, pp. 305–308.

[17] S. K. Mazumder, A. H. Nayfeh, and D. Boroyevich, "Theoretical and experimental investigation of the fast- and slow-scale instabilities of a DC-DC converter," *IEEE Trans. Power Electron.*, vol. 16, no. 2, pp. 201–216, 2001.

[18] S. K. Mazumder, A. H. Nayfeh, and D. Boroyevich, "A new approach to the stability analysis of boost power-factor-correction circuits," *J. Vib. Control*, vol. 9, pp. 749–773, 2003.

[19] Z. T. Zhusubaliyev, E. A. Soukhoterin, and E. Mosekilde, "Quasi-periodicity and border collision bifurcations in a DC-DC converter with pulsewidth modulation," *IEEE Trans. Circuits Syst. I, Fundam. Theory Appl.*, vol. 50, no. 8, pp. 1047–1057, 2003.

[20] Z. T. Zhusubaliyev, E. A. Soukhoterin, and E. Mosekilde, "Border-collision bifurcations on a two-dimensional torus," *Chaos, Solitons, Fractals*, vol. 13, pp. 1889–1915, 2002.

[21] Z. Zhusubaliyev and E. Mosekilde, "Torus birth bifurcations in a DC/DC converter," *IEEE Trans. Circuits Syst. I, Reg. Papers*, vol. 53, no. 8, pp. 1839–1850, Aug. 2006.

[22] F. Wang, H. Zhang, and X. Ma, "Analysis of slow-scale instability in boost PFC converter using the method of harmonic balance and floquet theory," *IEEE Trans. Circuits Syst. I, Reg. Papers*, vol. 57, no. 2, pp. 405–414, Feb. 2010.

[23] Y. Chen, C. K. Tse, S. C. Wong, and S.-S. Qiu, "Interaction of fast-scale and slow-scale bifurcations in current-mode controlled DC/DC converters," *Int. J. Bifurcation Chaos*, vol. 17, no. 5, pp. 1609–1622, 2007.

[24] Y. Chen, C. K. Tse, S.-S. Qiu, L. Lindenmuller, and W. Schwarz, "Coexisting fast-scale and slow-scale instability in current-mode controlled DC/DC converters: Analysis, simulation and experimental results," *IEEE Trans. Circuits Syst. I, Reg. Papers*, vol. 55, no. 10, pp. 3335–3348, Nov. 2008.

[25] D. Giaouris, S. Banerjee, B. Zahawi, and V. Pickert, "Stability analysis of the continuous conduction mode buck converter via Filippov's method," *IEEE Trans. Circuits Syst. I, Reg. Papers*, vol. 55, no. 4, pp. 1084–1096, May 2008.

[26] D. Giaouris, S. Maity, S. Banerjee, V. Pickert, and B. Zahawi, "Application of Filippov method for the analysis of subharmonic instability in DC–DC converters," *Int. J. Circuit Theory Appl.*, vol. 37, no. 8, pp. 899–919, 2009.

[27] D. Giaouris, S. Banerjee, B. Zahawi, and V. Pickert, "Control of fast scale bifurcations in power factor correction converter," *IEEE Trans. Circuits Syst. II, Exp. Briefs*, vol. 54, pp. 805–809, Sep. 2007.

[28] S. Newhouse, D. Ruelle, and F. Takens, "Occurrence of strange axiom A attractors near quasi periodic flows on T^m, $m \geq 3$," *Commun. Math. Phys.*, vol. 64, no. 1, pp. 35–40, 1978.

[29] G. Luo, Y. Chu, Y. Zhang, and J. Zhang, “Double Neimark-Sacker bifurcation and torus bifurcation of a class of vibratory systems with symmetrical rigid stops,” *J. Sound Vib.*, vol. 298, no. 1-2, pp. 154–179, 2006.

[30] G. Iooss and J. E. Los, “Quasi-genericity of bifurcations to high dimensional invariant tori for maps,” *Commun. Math. Phys.*, vol. 119, pp. 453–500, 1988.

[31] S. Mazumder, A. Nayfeh, and D. Boroyevich, “An investigation into the fast- and slow-scale instabilities of a single phase bidirectional boost converter,” *IEEE Trans. Power Electron.*, vol. 18, no. 4, pp. 1063–1069, 2003.

[32] M. di Bernardo, C. J. Budd, and A. R. Champneys, “Normal form maps for grazing bifurcations in n-dimensional piecewise-smooth dynamical systems,” *Physica D*, vol. 160, no. 3-4, pp. 222–254, 2001.

[33] M. di Bernardo, C. Budd, A. R. Champneys, and P. Kowalczyk, *Piecewise-Smooth Dynamical Systems*. London, U.K.: Springer-Verlag, 2008.

[34] K. Mandal, S. Banerjee, and C. Chakraborty, “Bifurcations in load resonant DC-DC converters,” in *Proc. IEEE Int. Symp. Circuits Syst. (ISCAS)*, 2010, pp. 133–136.

[35] C. Kaas-Petersen, “Computation, continuation, and bifurcation of torus solutions for dissipative maps and ordinary differential equations,” *Physica D*, vol. 25, pp. 288–306, 1987.

[36] R. Szalai and H. M. Osinga, “Arnol’d tongues arising from a grazing-sliding bifurcation,” *SIAM J. Appl. Dyn. Syst.*, vol. 8, no. 4, pp. 1434–1461, 2009.

[37] F. Schilder, H. M. Osinga, and W. Vogt, “Continuation of quasi-periodic invariant tori,” *SIAM J. Appl. Dyn. Syst.*, vol. 4, no. 3, pp. 459–488, 2005.

Damian Giaouris was born in Munich, Germany, in 1976. He received the Diploma degree of automation engineering from the Automation Department, Technological Educational Institute of Thessaloniki, Greece, in 2000, the M.Sc. degree in automation and control from Newcastle University, U.K., in 2001, and the Ph.D. degree in the area of control and stability of induction machine drives from Newcastle University, U.K., in 2004.

He is currently a Lecturer in Control Systems at Newcastle University, U.K. His research interests involve advanced nonlinear control, estimation, digital signal processing methods applied to electric drives, and nonlinear phenomena in power electronic converters.

Soumitro Banerjee (M’91–SM’02) was born in 1960. He received the B.E. degree from the Bengal Engineering College, Calcutta University, India, in 1981 and the M.Tech. and Ph.D. degrees from IIT Delhi, India, in 1983 and 1987, respectively.

He was in the faculty of the IIT Kharagpur since 1986, before moving to the Indian Institute of Science Education & Research—Kolkata, India, in 2009. He has published three books: *Nonlinear Phenomena in Power Electronics* (Eds. Banerjee and Verghese, IEEE Press, 2001), *Dynamics for Engineers* (Wiley, London, 2005), and *Wind Electrical Systems* (Oxford University Press, New Delhi, 2005). His areas of interest are the nonlinear dynamics of power electronic circuits and systems, and bifurcation theory for nonsmooth systems.

Dr. Banerjee is a Fellow of the Indian Academy of Sciences, the Indian National Academy of Engineering, and the Indian National Science Academy. He is a recipient of the S. S. Bhatnagar Prize (2003), and is recognized as a “Highly Cited Author” (http://www.isihighlycited.com/). He served as Associate Editor of the IEEE TRANSACTIONS ON CIRCUITS AND SYSTEMS—PART II (2003–2005), and Associate Editor of the IEEE TRANSACTIONS ON CIRCUITS AND SYSTEMS—PART I (2006–2007).

Otman Imrayed was born in Nofalia, Libya, on May 2, 1965. He received the B.Sc. degree in electrical and electronic engineering from the Bright Star University of Technology, Libya, in 1989 and the M.Sc. degree in automatic control from the AGH University of Science and Technology, Poland, in 1999. He is currently working toward the Ph.D. degree from Newcastle University, U.K.

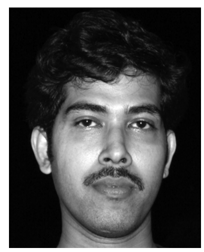

Kuntal Mandal received the B.E. degree in electrical engineering from the Jalpaiguri Govertment Engineering College, North Bengal University, West Bengal, India, in 2003 and the M.E. degree in control system engineering from Jadavpur University, Kolkata, India, in 2006. He is currently working toward the Ph.D. degree at the Department of Electrical Engineering, Indian Institute of Technology, Kharagpur (IIT Kharagpur), India.

His research interests include nonlinear dynamics of power electronic circuits and its control.

Bashar Zahawi (M’96–SM’04) received the B.Sc. and Ph.D. degrees in electrical and electronic engineering from Newcastle University, U.K., in 1983 and 1988, respectively.

From 1988 to 1993 he was a design engineer at Cortina Electric Company Ltd, a U.K. manufacturer of large ac variable speed drives and other power conversion equipment. In 1994, he was appointed as a Lecturer in Electrical Engineering at the University of Manchester, U.K., and in 2003 he joined the School of Electrical, Electronic & Computer Engineering at Newcastle University, U.K., as a Senior Lecturer. His research interests include power conversion, variable speed drives, and the application of nonlinear dynamical methods to transformer and power electronic circuits.

Dr. Zahawi is a Chartered Electrical Engineer and a recipient of the Crompton premium awarded by the IEE.

Volker Pickert (S’94–A’98–M’04) studied electrical and electronic engineering at the RWTH Aachen and the University of Cambridge, and received the Dipl.-Ing. degree in 1994. He received the Ph.D. degree from Newcastle University, U.K., in the area of power electronics in 1997.

After his Ph.D. he worked for two years as an application engineer for Semikron International and for five years as project manger for Volkswagen, where he was responsible for power electronic systems and electric drives for electric and hybrid electric vehicles. Since 2003 he has been Senior Lecturer at Newcastle University, U.K. His research interests are power electronics in automotive applications, thermal management, fault tolerant power converters, and nonlinear controllers.